Published in final edited form as:

Neuroreport. 2023 November 01; 34(16): 786–791. doi:10.1097/WNR.0000000000001953.

Prenatal Zika virus exposure is associated with lateral geniculate nucleus abnormalities in juvenile rhesus macaques

Erin E. Ball[1,4,5], **Jeffrey Bennett**[2,3], **Rebekah I. Keesler**[2,6], **Koen K. A. Van Rompay**[1,2], **Lark L. Coffey**[1], **Eliza Bliss-Moreau**[2,3]

[1]Department of Pathology, Microbiology and Immunology, University of California, Davis, CA, USA

[2]California National Primate Center, University of California, Davis, CA, USA

[3]Department of Psychology, University of California, Davis, CA, USA

[4]United States Army, Veterinary Corps

[5]Currently Armed Forces Research Institute of Medical Sciences (AFRIMS), Bangkok, Thailand

[6]Currently Charles River Laboratories, Reno, NV

Abstract

Objectives: Zika virus' neural tropism causes significant neural pathology, particularly in developing fetuses. One of the consistent findings from humans and animal models is that prenatal exposure to Zika virus (ZIKV) causes pathology in the eyes and visual pathways of the brain, although the extent to which this pathology persists over development is not clear. In the present report, we build upon our previous work which demonstrated that full term rhesus monkey (*Macaca mulatta*) fetuses who were exposed to ZIKV early in gestation had significant pathological abnormalities to the organization of the lateral geniculate nucleus (LGN), a major hub of the visual network. The objective of the present work was to replicate those LGN findings and determine whether such pathology persisted across childhood development.

Methods: We carried out histological analyses of the LGNs of two juvenile rhesus monkeys who were prenatally exposed to ZIKV and two age-matched controls. Pregnant rhesus monkeys were infected with ZIKV via the intravenous and intra-amniotic routes and tracked across development. Following sacrifice and perfusion, brains were subjected to quantitative neuroanatomical analyses with a focus on the size and structure of the LGN and its composite layers.

Results: Early fetal ZIKV exposure resulted in developmental abnormalities within the brains' visual pathway: specifically disorganization, blending of layers, laminar discontinuities, and regions of low cell density within the LGN. These abnormalities were not observed in the control animals.

Corresponding authors: eblissmoreau@ucdavis.edu, California National Primate Research Center, Davis, California 95616 USA, 530-752-6268, lcoffey@ucdavis.edu, Department of Pathology, Microbiology and Immunology, School of Veterinary Medicine, University of California, Davis, Davis, California 95616 USA, 530-752-2946.

Disclosures: The authors do not declare any conflict of interest. Funding sources did not influence experimental design and analysis/interpretation of results or impact the decision to publish.

Conclusions: Our findings demonstrates that the ZIKV's damage to the LGN that occurs during fetal development persists into childhood.

Keywords

Zika virus; prenatal Zika virus exposure; congenital Zika syndrome; juvenile rhesus macaque; lateral geniculate nucleus defect; CNS developmental abnormality

Introduction

Zika virus (ZIKV) infection in pregnant women can result in fetuses developing congenital Zika syndrome (CZS). CZS includes both pathology in utero, such as pathological alterations to the placenta, premature rupture of membranes, fetal growth restriction, musculoskeletal contracture, and fetal central nervous system (CNS) malformations, including microcephaly, small cerebral cortices, retinal lesions, hearing loss, and early fetal death [1]. Data indicate that ZIKV is neurotropic, targeting embryonic neural progenitor cells (NPCs) in the developing brain, which can result in NPC transcriptional dysregulation, decreased cell migration, impaired neurogenesis and cell death, with defective cortical development and congenital defects reminiscent of CZS [2–7]. A significant number of newborns born to mothers whom had been infected with ZIKV were born with microcephaly [8], but even normocephalic newborns with confirmed ZIKV infection but no observable congenital defects developed neurologic deficits and behavioral abnormalities consistent with CZS [9]. These neurobiological components of CZS are not well understood and the focus of the present experiment (detailed in Figure 1).

Research since the onset of the 2015/2016 ZIKV pandemic has illustrated that ZIKV's neural tropism, and particular affinity for neural progenitors, can cause significant brain-wide neuropathology in developing fetuses (for a review see [10]). One of the consistent observations in human infants with CZS is the disruption of the visual pathways and processing, including ocular pathology and vision impairments [11–13]. In a highly translatable animal model for human disease processes and vision-related anatomy, the rhesus monkey (Macaca mulatta), we recently demonstrated that visual pathway pathology in monkeys exposed to ZIKV in utero is not limited to the eye but also includes abnormalities to brain hubs that process visual information, namely the lateral geniculate nucleus [14]. The LGN is a 6-layered structure in the ventral thalamus, which receives spatially organized retinal input from the optic tract and projects to the primary visual cortex of the occipital lobe (Figure 1B–C) [15]. We demonstrated that in full term rhesus fetuses, early exposure to ZIKV in utero disrupted the layered organization of the LGN [16], consistent with observations in mouse models (e.g., [17; 18]). This disruption may have occurred via direct infection or the neuroinflammatory response to infection that persisted until sacrifice [16]. Alternatively LGN pathology may have occurred via the development of retinal pathology early in development that is critical for the normal development of the LGN (for a review [19]). To date, macaque studies evaluating neuroanatomical abnormalities associated with CZS have assessed fetuses or animals sacrificed shortly after birth [20–24]; the consequences of prenatal ZIKV infection beyond infancy remain largely unknown.

In the present report, we evaluated the structural anatomy of the LGN in a cohort of juvenile rhesus monkeys who were exposed to ZIKV in utero, and compared those anatomical features to age-matched control monkeys who had not been exposed to ZIKV (Fig 1). We tested the hypothesis that the LGN pathology we observed in full term fetuses [14] would persist into childhood. Specially, we carried out histological evaluations of the LGN in two two-year old monkeys who had been exposed to ZIKV in utero via intra-amniotic inoculations and intravenous inoculations of their mothers. Their brains were compared to those of age-matched controls who had not been ZIKV exposed. One of the ZIKV exposed infants was determined to have retinal pathology prior to sacrifice that was confirmed histologically [25], supporting the idea that ZIKV induced pathology to visual pathways in utero persists across development.

Methods

Study Approval

All work adhered to the 2011 NIH Guide for the Care and Use of Laboratory Animals and was conducted on protocols #19211 and 20959 approved by the IACUC at University of California, Davis, which is accredited by the Association for Assessment and Accreditation of Laboratory Animal Care (AAALAC).

Study Design

Using a previously validated model of CZS [20], 6 pregnant rhesus macaque dams were inoculated intravenously (IV) and intra-amniotically (IA) with ZIKV between gestation days (GD) 42 and 53, which, given the macaque gestation period of approximately 165–170 days [26], corresponds to the first trimester of pregnancy. Inoculation occurred both intravenously and intra-amniotically with a combination of 1000 plaque forming units (PFU) of Puerto Rico 2015 ZIKV (PRVABC-59; GenBank, KU501215) and 1000 PFU of Brazil 2015 (Zika virus/H.sapiens-tc/BRA/2015/Brazil_SPH2015; GenBank, KU321639.1) on GD 51 (Dam 1) or GD 53 (Dam 2). This dual route inoculation was used to ensure that fetuses were exposed to ZIKV, given that vertical transmission from mother to fetus is not entirely certain (e.g., a recent study documented no vertical transmission [27]).

Dams exhibited prolonged viremia with detection of ZIKV RNA in amniotic fluid samples throughout gestation and adverse fetal outcomes (e.g., early fetal death) in 4 of 6 dams [28]. ZIKV RNA was isolated from placenta and fetal brain [28], implicating ZIKV as the underlying etiology. Each of the 2 remaining pregnant dams (Dam 1 and Dam 2) gave birth to a live female (Subject 1 and Subject 2) by natural delivery on GD 168 or 171, respectively (Figure 1).

Subjects 1 and 2 had normal birth weight (460 g and 500 g, respectively, where the mean birth weight of captive colony-born female macaques is reported as 488 g [29]) and normal body measurements relative to archived data from other newborn macaques at the facility [28]. There was no gross or ultrasonographic evidence of microcephaly, defined as a biparietal diameter ≥ 2 standard deviations below the colony mean [28]. Both neonates had detectable anti-ZIKV IgG titers which gradually declined to undetectable levels, suggesting

passive transfer of maternal anti-ZIKV antibody and lack of postnatal viral replication [28]. Subjects 1 and 2 were maternally reared for 17 months and then pair-housed with regular clinical monitoring, including physical, ophthalmologic, and neurologic examinations. Physical exams and routine bloodwork remained normal, and serial blood (≥15 time points), urine, and CSF samples failed to yield detectable ZIKV RNA [28]. Neither animal exhibited any obvious postnatal behavioral or neurological defects. Overall eye growth appeared normal; however, Subject 1 developed postnatal ocular abnormalities characterized by bilateral, progressive colobomatous chorioretinal atrophic lesions, previously described by Yiu *et al.* [28]. Two age-matched, nursery-reared, juvenile male macaques not exposed to ZIKV served as controls.

All 4 juvenile macaques were humanely euthanized at 2-years-old, with post-mortem examination and collection of tissue and fluid samples as previously described [28]. ZIKV RNA was not detected in spleen or inguinal lymph node of the Zika-exposed infants [28], indicating the absence of current infection. There were no significant macro- or microscopic abnormalities in the spleen, lymph nodes, lung, heart, jejunum, liver, kidney, spinal cord, or middle ear of any examined animal [28].

Tissue processing

Processing and analysis of paraformaldehyde-fixed, Nissl-stained tissues sections is described in depth by Beckman *et al.* [16]. In contrast to that methodology, where fetal brain hemispheres were immersion fixed, in these studies the upper body was perfused with 4% paraformaldehyde (EMS, Hatfield, PA USA) in 0.1 M sodium phosphate buffer (ThermoFisher) for optimal preservation of brains and eyes. The left brain hemisphere and other tissues were fixed in 10% neutral buffered formalin (NBF) (ThermoFisher), paraffin-embedded, thin-sectioned (5 μm), stained with hematoxylin and eosin (H&E), and evaluated by board-certified veterinary pathologists (EEB, RIK). The right hemisphere and both eyes were fixed in 4% paraformaldehyde for 48 hours, cryoprotected in 10% glycerin (ThermoFisher) with 2% DMSO (Sigma-Aldrich, St Louis, MO USA) in 0.1 M sodium phosphate buffer overnight, then 20% glycerin with 2% DMSO in 0.1 M sodium phosphate buffer (PB) for 72 hours. Tissues were then frozen in isopentane (ThermoFisher) and sectioned on a sliding freezing microtome (ThermoFisher, Microm HM430) into 8 series (7 at 30 μm and 1 at 60 μm). 30 μm tissue sections were placed in a cryoprotectant solution (Ethylene glycol, glycerin in 0.1 M phosphate buffer) and stored at −20°C. 60 μm tissue sections were post-fixed for 2 weeks in 10% NBF and stored at 4°C, then rinsed in PB, mounted on gelatin subbed slides, Nissl stained using 0.25% thionin (ThermoFisher) and cover-slipped using DPX mounting medium (Millipore Sigma, St. Louis, MO USA). Nissl-stained sections were scanned (TissueScope LE; Huron Digital Pathology; St. Jacobs, ON Canada) and digital images were used for blinded analyses.

Analysis of the LGN

Blinded digital images were processed using ImageJ (Fiji, NIH). Anatomical analyses were performed on the 3 largest complete sections of LGN from each subject. The total LGN surface area in each section and then the magnocellular (layers 1 and 2) and parvocellular (layers 3 – 6) surface areas were measured 3 times. The koniocellular surface area was

calculated as the total LGN surface area minus the magnocellular and parvocellular areas. Measurements were averaged for each animal. Mean values for each metric are presented descriptively but no statistical analyses were performed because of the extremely small sample size.

Results

Using serial Nissl-stained sections of brain and image analysis software (ImageJ, Fiji, NIH), we computed the proportion of LGN surface area occupied by the magno-, parvo- and koniocellular layers for comparison between ZIKV-exposed and age-matched controls (see Figure 2 for normal LGN anatomy). Descriptive statistics suggested that, while mean whole areas were comparable between controls and prenatally ZIKV-exposed macaques, there was decreased parvocellular and increased koniocellular surface area in prenatally ZIKV-exposed animals compared to controls (Figure 3A). Microscopic evaluation of Nissl-stained sections of brain from Subjects 1 and 2 revealed structural abnormalities within the LGN comparable to those previously reported in fetal brains [16] (Figure 3B and C). The 2 control animals appeared normal.

Normally, the magno- and parvocellular layers of the LGN are separated by a thin layer of koniocellular tissue (Figure 2). However, in Subjects 1 and 2 there was blurring of these boundaries, laminar discontinuities, and regions of low cell density, particularly affecting the rostral portion of the LGN. In Subject 1 these defects occurred primarily within the parvocellular layers at the level of the hilum (Figure 3B), while the ventrolateral aspect of the magnocellular layers was more severely affected in Subject 2 (Figure 3C). There was no overt pathology observed in the visual cortices (V1) of any of the subjects.

Discussion

We observed pathology in the LGN of two juvenile rhesus monkeys following fetal exposure to Zika virus that was not present in non-exposed juveniles. This pathology was consistent with our recently reported findings in full term fetal macaques from a similar cohort of animals exposed to ZIKV in the first or second trimester; neuroanatomical evaluation of specific brain regions revealed a number of macrostructural neurodevelopmental abnormalities within the cerebral cortex, including the LGN [16]. Lesions within the visual system appear to be a consistent feature of CZS in both humans [11–13] and animal models [16–18; 24]. Proper anatomic and functional organization of the LGN, is present at birth but continues to develop postnatally and is critical for normal neural and ocular development [15; 30].

Notably, in addition to the neuroanatomic abnormalities within both subjects' LGN, Subject 1 exhibited postnatal ocular developmental lesions, including retinal pathology, but Subject 2 did not which was detailed in a previously published report [28]. This combination of effects leads to new hypotheses about the mechanism by which LGN pathology arises after ZIKV exposure. Decades of research demonstrates that the organization and function of the LGN is retinal dependent and that spontaneous activity of the retina in utero, before sight, is a critical part of this process (for a review [19]). Given the structural pathology of the LGN,

in combination with an increased presence of microglia and astrocytes in our ZIKV exposed fetuses from our previous work [14], we reasoned that it likely resulted from direct infection and/or associated immune responses of the structure. Another possible hypothesis was that ZIKV acted on the retinas which had upstream consequences for LGN development. The latter hypothesis becomes less likely given that retinal pathology was observed in only one subject but LGN pathology was observed in both. Regardless of mechanism, these findings are consistent with published reports of delayed childhood neurodevelopment and neurosensory alterations in infants and children prenatally exposed to ZIKV, where language function, vision and hearing, cognition, and motor function can all be impacted [9; 31; 32]. While we previously observed some pathology of visual cortex in fetuses exposed to Zika virus [16], no notable pathology was present in the current cases, perhaps because of neural plasticity and reorganization following birth. Unfortunately, the tissue preparation prevented us from carrying out quantitative analyses of visual cortex, although our qualitative review of available tissue sections indicated normality of visual cortex.

Lack of power due to the small sample size in this descriptive study precludes robust statistical analysis or evaluation of significant differences of magno-, parvo- and koniocellular surface area between controls and ZIKV-exposed fetuses; however, there is clear association between prenatal ZIKV exposure and structural neurodevelopmental abnormalities in the LGN which warrants further investigation. Additionally, controlled experiments evaluating the long-term neurologic consequences of both prenatal and postnatal ZIKV infection are undoubtedly needed. To our knowledge, this is the first description of postnatal neuroanatomical defects in normocephalic macaques 2 years after fetal ZIKV exposure. Our findings may help explain why some prenatally ZIKV exposed normocephalic newborns who exhibit no grossly observable congenital defects exhibit ocular lesions and visual deficits as juveniles.

In summary, this work demonstrates that fetal ZIKV exposure can generate neuroanatomical abnormalities that persist into childhood in a rhesus macaque model of ZIKV infection. These abnormalities include disorganization, blending of layers, laminar discontinuities, and regions of low cell density in the LGN. The extent to which these cellular-level pathologies result in functional pathologies (e.g., compromise to vision) is a target of future research. Whether or not this neuropathology has consequences for visual acuity is not known, and an important avenue for future research.

Funding:

NIH Award Numbers: R01 HD096436 (EBM), R21 NS104692 (EBM), R21AI129479 (KKAVR), Office of Research Infrastructure Program P51OD011107 (CNPRC) and T32 OD 011147 (EEB); U.C. Davis Graduate Student Support Program (EEB); U.S. Army Long Term Health Education & Training Program (EEB).

References

1. Weaver SC, Costa F, Garcia-Blanco MA, Ko AI, Ribeiro GS, Saade G, et al. Zika virus: History, emergence, biology, and prospects for control. Antiviral Research 2016; 130: 69–80. [PubMed: 26996139]

2. Cugola FR, Fernandes IR, Russo FB, Freitas BC, Dias JLM, Guimarães KP, et al. The Brazilian Zika virus strain causes birth defects in experimental models. Nature 2016; 534 (7606): 267–271. [PubMed: 27279226]

3. Dang J, Tiwari SK, Lichinchi G, Qin Y, Patil VS, Eroshkin AM, et al. Zika Virus Depletes Neural Progenitors in Human Cerebral Organoids through Activation of the Innate Immune Receptor TLR3. Cell Stem Cell 2016; 19 (2): 258–265. [PubMed: 27162029]

4. Zhang N, Zhang N, Qin CF, Liu X, Shi L, Xu Z. Zika Virus Disrupts Neural Progenitor Development and Leads to Microcephaly in Mice. Cell Stem Cell 2016; 19: 120–126. [PubMed: 27179424]

5. Shao Q, Herrlinger S, Yang S-L, Lai F, Moore JM, Brindley MA, et al. Zika virus infection disrupts neurovascular development and results in postnatal microcephaly with brain damage. Development 2016; 143: 4127–4136. [PubMed: 27729407]

6. Wu KY, Zuo GL, Li XF, Ye Q, Deng YQ, Huang XY, et al. Vertical transmission of Zika virus targeting the radial glial cells affects cortex development of offspring mice. Cell Research 2016; 26 (6): 645–654. [PubMed: 27174054]

7. Tang H, Hammack C, Ogden SC, Wen Z, Qian X, Li Y, et al. Zika virus infects human cortical neural progenitors and attenuates their growth. Cell Stem Cell 2016; 18 (5): 587–590. [PubMed: 26952870]

8. Rasmussen SA, Jamieson DJ, Honein MA, Petersen LR. Zika Virus and Birth Defects — Reviewing the Evidence for Causality. New England Journal of Medicine 2016; 374 (20): 1981–1987. [PubMed: 27074377]

9. Cardoso TF, Santos RS Dos, Corrêa RM, Campos JV, Silva RDB, Tobias CC, et al. Congenital Zika infection: Neurology can occur without microcephaly. Archives of Disease in Childhood 2019; 104 (2): 199–200. [PubMed: 29858269]

10. Christian KM, Song H, Ming G. Pathophysiology and Mechanisms of Zika Virus Infection in the Nervous System. Annual Review of Neuroscience 2019; 42 (1): 249–269.

11. Ventura C V, Ventura LO, Bravo-Filho V, Martins TT, Berrocal AM, Gois AL, et al. Optical coherence tomography of retinal lesions in infants with congenital zika syndrome. JAMA Ophthalmology 2016; 134 (12): 1420–1427. [PubMed: 27832267]

12. Miranda HA de Costa MC, Frazão MAM, Simão N, Franchischini S, Moshfeghi DM. Expanded Spectrum of Congenital Ocular Findings in Microcephaly with Presumed Zika Infection. Ophthalmology 2016; 123 (8): 1788–1794. [PubMed: 27236271]

13. De Paula Freitas B, De Oliveira Dias JR, Prazeres J, Sacramento GA, Ko AI, Maia M, et al. Ocular findings in infants with microcephaly associated with presumed zika virus congenital infection in Salvador, Brazil. JAMA Ophthalmology 2016; 134 (5): 529–535. [PubMed: 26865554]

14. Beckman D, Seelke AMH, Bennett J, Dougherty P, Van Rompay KKA, Keesler R, et al. Neuroanatomical abnormalities in a nonhuman primate model of congenital Zika virus infection. Elife 2022; 11: e64734. [PubMed: 35261339]

15. De Moraes CG. Anatomy of the visual pathways. Journal of Glaucoma 2013; 22 (5 SUPPL.1): 2–7.

16. Beckman D, Seelke AM, Bennett J, Dougherty P, Rompay KA Van, Keesler R, et al. Neuroanatomical abnormalities in a nonhuman primate model of congenital Zika virus infection. bioRxiv 2020; 2020.11.10.374611.

17. van den Pol AN, Mao G, Yang Y, Ornaghi S, Davis JN. Zika virus targeting in the developing brain. J Neurosci 2017;

18. Noguchi KK, Swiney BS, Williams SL, Huffman JN, Lucas K, Wang SH, et al. Zika Virus Infection in the Developing Mouse Produces Dramatically Different Neuropathology Dependent on Viral Strain. J. Neurosci. 2020; 40 (5): 1145–1161. [PubMed: 31836659]

19. Stacy AK, Van Hooser SD. Development of Functional Properties in the Early Visual System: New Appreciations of the Roles of Lateral Geniculate Nucleus. In: Andersen SL (ed). Sensitive Periods of Brain Development and Preventive Interventions. Cham: Springer International Publishing; 2022. pp. 3–35.

20. Coffey LL, Keesler RI, Pesavento PA, Woolard K, Singapuri A, Watanabe J, et al. Intraamniotic Zika virus inoculation of pregnant rhesus macaques produces fetal neurologic disease. Nature Communications 2018; 9 (1): 1–12.
21. Adams Waldorf KM, Stencel-Baerenwald JE, Kapur RP, Studholme C, Boldenow E, Vornhagen J, et al. Fetal Brain Lesions After Subcutaneous Inoculation of Zika Virus in a Pregnant Nonhuman Primate. Nature Medicine 2016; 22 (11): 1256–1259.
22. Adams Waldorf KM, Nelson BR, Stencel-Baerenwald JE, Studholme C, Kapur RP, Armistead B, et al. Congenital Zika virus infection as a silent pathology with loss of neurogenic output in the fetal brain. Nature Medicine 2018; 24 (3): 368–374.
23. Martinot AJ, Abbink P, Afacan O, Prohl AK, Bronson R, Hecht JL, et al. Fetal Neuropathology in Zika Virus-Infected Pregnant Female Rhesus Monkeys. Cell 2018; 173 (5): 1111–1122.e10. [PubMed: 29606355]
24. Mohr EL, Block LN, Newman CM, Stewart LM, Koenig M, Semler M, et al. Ocular and uteroplacental pathology in a macaque pregnancy with congenital Zika virus infection. PLoS ONE 2018; 13 (1):
25. Yiu G, Thomasy SM, Casanova MI, Rusakevich A, Keesler RI, Watanabe J, et al. Evolution of ocular defects in infant macaques following in utero Zika virus infection. JCI Insight 2020; 5 (24):
26. Carter AM. Animal Models of Human Placentation - A Review. Placenta 2007; 28 (SUPPL.): S41–S47. [PubMed: 17196252]
27. Dudley DM, Koenig MR, Stewart LM, Semler MR, Newman CM, Shepherd PM, et al. Human immune globulin treatment controls Zika viremia in pregnant rhesus macaques. PLoS One 2022; 17 (7): e0266664. [PubMed: 35834540]
28. Yiu G, Thomasy SM, Isabel Casanova M, Rusakevich A, Keesler RI, Watanabe J, et al. Evolution of ocular defects in infant macaques following in utero Zika virus infection. JCI Insight 2020; 5 (24):
29. Hopper KJ, Capozzi DK, Newsome JT. Effects of maternal and infant characteristics on birth weight and gestation length in a colony of rhesus macaques (macaca mulatta). Comparative Medicine 2008; 58 (6): 597–603. [PubMed: 19149417]
30. Garey L, De Courten C. Structural development of the lateral geniculate nucleus and visual cortex in monkey and man. Behavioural Brain Research 1983; 10 (1): 3–13. [PubMed: 6639728]
31. Peçanha PM, Gomes Junior SC, Pone SM, Pone MV da S, Vasconcelos Z, Zin A, et al. Neurodevelopment of children exposed intra-uterus by Zika virus: A case series. PloS one 2020; 15 (2): e0229434. [PubMed: 32109947]
32. Nielsen-Saines K, Brasil P, Kerin T, Vasconcelos Z, Gabaglia CR, Damasceno L, et al. Delayed childhood neurodevelopment and neurosensory alterations in the second year of life in a prospective cohort of ZIKV-exposed children. Nature Medicine 2019;

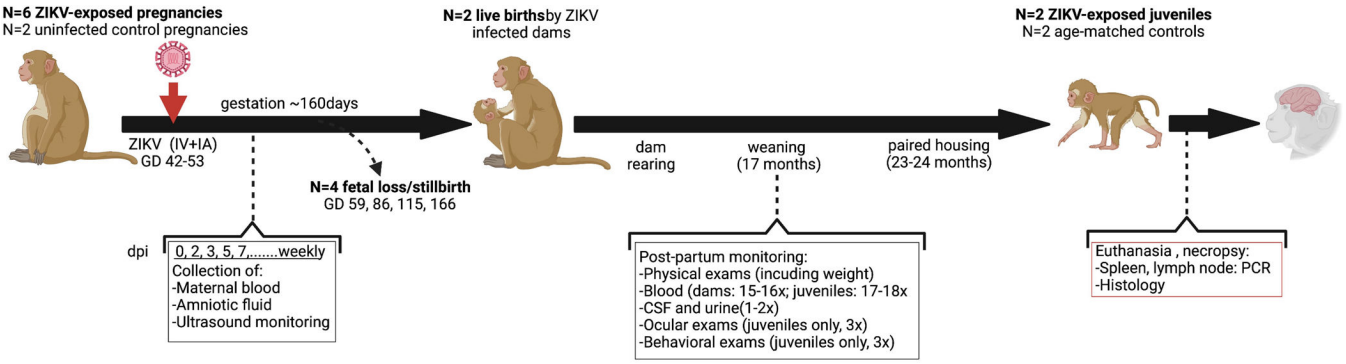

Figure 1. Experimental design.

GD = gestation day; dpi = days post-inoculation; CSF = cerebral spinal fluid, IV= intravenous, IA = intraamniotic. Adapted from Yiu, *et al.* (20) using BioRender.com.

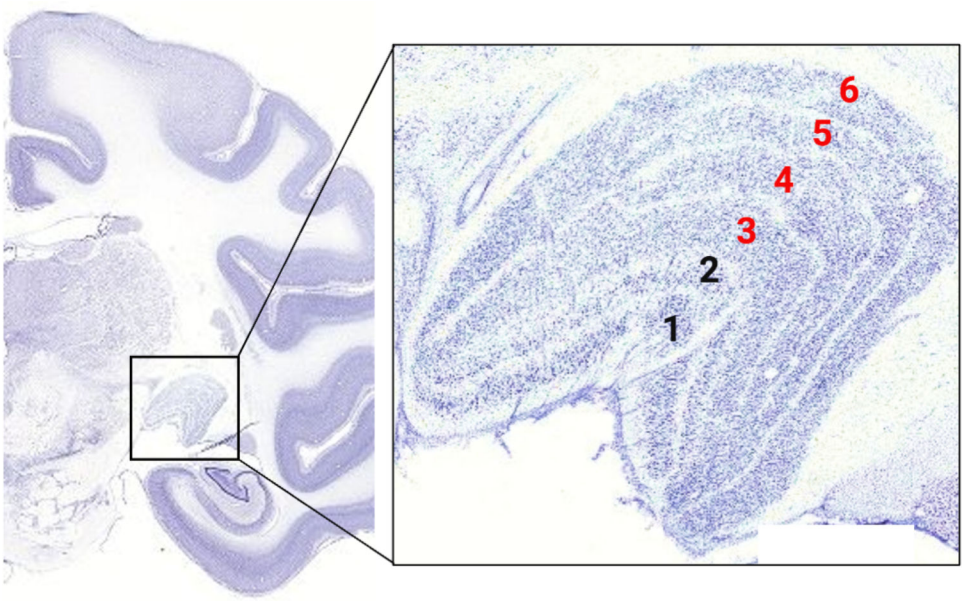

Figure 2. Normal anatomy of the lateral geniculate nucleus (LGN).

Nissl-stained coronal section of normal rhesus macaque brain depicting anatomic location of the LGN (box). Boxed area is a normal Nissl-stained section of LGN with layers labeled as follows: 1 – 2 = magnocellular layers (contra- and ipsilateral inputs, respectively); 3 – 6 = parvocellular layers (alternating ipsi- and contralateral inputs). Magno- and parvocellular layers are separated by koniocellular tissue. Adapted from www.blueprintnhpatlas.org using BioRender.com.

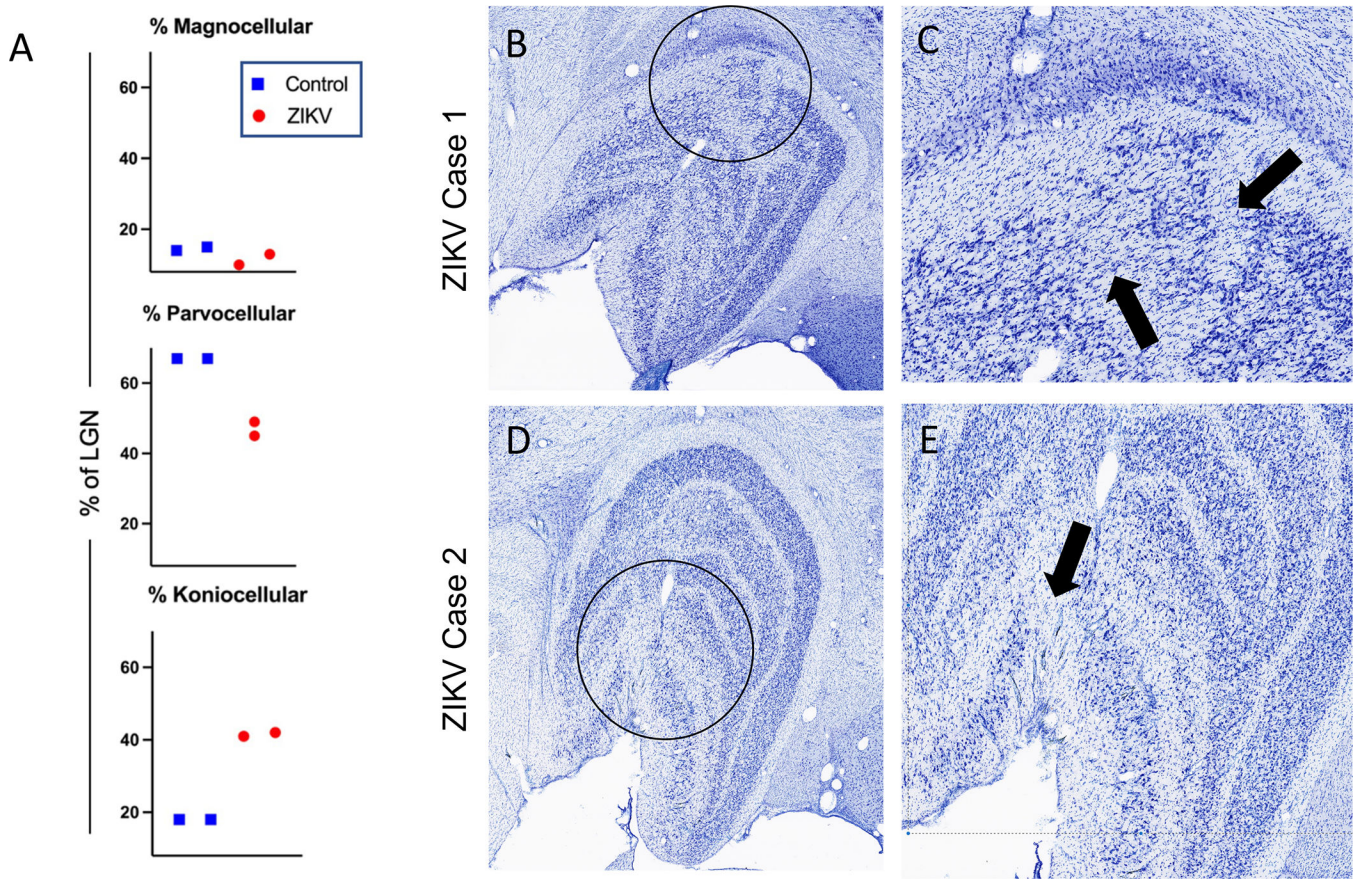

Figure 3. Pathology to the LGN of ZIKV exposed monkeys.

(A) The mean proportion of LGN surface area occupied by magno-, parvo- and koniocellular layers and calculated using ImageJ was comparable between controls and prenatally ZIKV-exposed juvenile macaques, with a trend toward decreased parvocellular and increased koniocellular surface area in both prenatally ZIKV-exposed animals. A representative slice depicting the pathology of ZIKV Cases 1 (B and C) and 2 (D and E) are presented with a view of the whole LGN (B and D) with pathological areas circled in black and then magnified in C and E. Black arrows in C and E point to areas of undifferentiated lamination with blending of layers and/or laminar discontinuities. Note also the variation in cell density in those regions.